The computational power of multi-particle quantum walk

Andrew Childs David Gosset Zak Webb

arXiv:1205.3782, Science **339**, 791-794 (2013)
arXiv:1311.3297

Quantum walk

Quantum analog of a random walk on a graph.

Idea: Replace probabilities by quantum amplitudes.
Interference can produce radically different behavior!

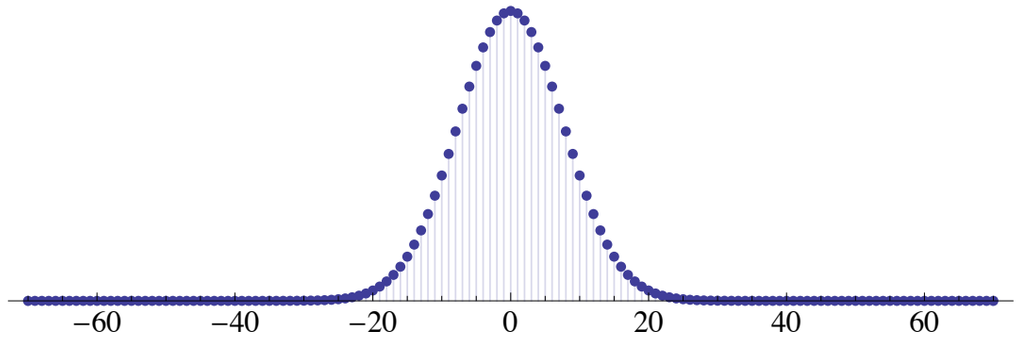

classical

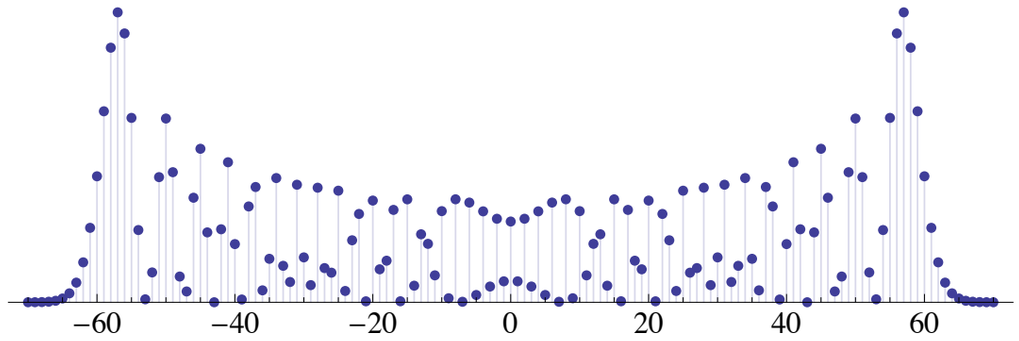

quantum

Quantum walk algorithms

Quantum walk is a major tool for quantum algorithms (especially query algorithms with polynomial speedup).

- Exponential speedup for black-box graph traversal [CCDFGS 02]
- Quantum walk search framework [Szegedy 05], [Magniez et al. 06]
  - Spatial search [Shenvi-Kempe-Whaley 02], [CG 03, 04], [Ambainis-Kempe-Rivosh 04]
  - Element distinctness [Ambainis 03]
  - Subgraph finding [Magniez, Santha, Szegedy 03], [CK 10]
  - Matrix/group problems [Buhrman, Špalek 04], [Magniez, Nayak 05]
- Evaluating formulas/span programs
  - AND-OR formula evaluation [Farhi, Goldstone, Gutmann 07], [ACRŠZ 07]
  - Span programs for general query problems [Reichardt 09]
  - Learning graphs [Belovs 11] → new upper bounds (implicitly, quantum walk algorithms), new kinds of quantum walk search

Continuous-time quantum walk

Quantum analog of a random walk on a graph $G = (V, E)$.

Idea: Replace probabilities by quantum amplitudes.

$$|\psi(t)\rangle = \sum_{v \in V} a_v(t)|v\rangle$$

amplitude for vertex v at time t

Define time-homogeneous, local dynamics on G.

$$\mathrm{i}\frac{\mathrm{d}}{\mathrm{d}t}|\psi(t)\rangle = H|\psi(t)\rangle$$

Adjacency matrix: $H = A(G) = \sum_{(u,v)\in E(G)} |u\rangle\langle v|$

Multi-particle quantum walk

With m distinguishable particles:

states: $|v_1, \ldots, v_m\rangle$ $\quad v_i \in V(G)$ Hilbert space dimension: n^m

Hamiltonian: $H_G^{(m)} = \sum_{i=1}^{m} A(G)_i + \mathcal{U}$

Indistinguishable particles:

bosons: symmetric subspace fermions: antisymmetric subspace

Many possible interactions:

on-site: $\mathcal{U} = J \sum_{v \in V(G)} \hat{n}_v(\hat{n}_v - 1)$ $\quad \hat{n}_v = \sum_{i=1}^{m} |v\rangle\langle v|_i$

(with bosons, this is the *Bose-Hubbard model*)

nearest-neighbor: $\mathcal{U} = J \sum_{(u,v) \in E(G)} \hat{n}_u \hat{n}_v$

Dynamics are universal; ground states are hard

Theorem: Any n-qubit, g-gate quantum circuit can be simulated by a multi-particle quantum walk of $n+1$ particles interacting for time $\mathrm{poly}(n,g)$ on an unweighted graph with $\mathrm{poly}(n,g)$ vertices.

Consequences:

- Architecture for a quantum computer with no time-dependent control
- Simulating dynamics of interacting many-body systems is BQP-hard (e.g., Bose-Hubbard model on a sparse, unweighted, planar graph)

Theorem: Approximating the ground energy of the n-particle Bose-Hubbard model on a graph is QMA-complete.

Consequences:

- Computing the ground energy of the Bose-Hubbard model is (probably) intractable
- New techniques for quantum Hamiltonian complexity

… but not always

model	dynamics	ground energy
Local Hamiltonians	BQP-complete	QMA-complete
Bose-Hubbard model (positive hopping)	BQP-complete	QMA-complete
stoquastic Local Hamiltonians	BQP-complete	AM
Bose-Hubbard model (negative hopping)	BQP-complete	AM
ferromagnetic Heisenberg model on a graph	BQP-complete	trivial

Universal computation by multi-particle quantum walk

arXiv:1205.3782, Science **339**, 791-794 (2013)

Universality of quantum walk

Quantum walk can be efficiently simulated by a universal quantum computer.

N-vertex graph		circuit with
max degree $\mathrm{poly}(\log N)$	$\Rightarrow$	$\mathrm{poly}(\log N)$ qubits
efficiently computable neighbors		$\mathrm{poly}(\log N)$ gates

Conversely, quantum walk is a *universal computational primitive*: any quantum circuit can be simulated by a quantum walk. [Childs 09]

		graph with
N dimensions		$\mathrm{poly}(N, g)$ vertices
g gates	$\Rightarrow$	max degree 3
		walk for time $\mathrm{poly}(g)$

Note: The graph is necessarily exponentially large in the number of qubits! Vertices represent basis states.

Single-particle quantum walk experiments

Experimental realization of a quantum quincunx by use of linear optical elements

Department

School of E

lation between brightness and vertical flow direction (*12*). This constitutes evidence for a convective flow pattern that transports the energy flux emitted in the penumbra. Other studies show a correlation between intensity and line-of-sight velocities (*13*), which for sunspots observed outside the center of the solar disk is dominated by the horizontal Evershed flow. This is consistent with our findings, because in the penumbra the horizontal flow velocity is correlated with the vertical flow direction.

Our detailed analysis (*8*) shows that the spatial scales of the flows providing the major part of the convective energy transport are similar for both undisturbed granulation and penumbra. The primary difference is that there is no preferred horizontal direction for granulation, whereas the energy-transporting flows in the penumbra are distinctly asymmetric: Convective structures are elongated in the radial direction of the sunspot. These properties were already indicated in earlier simulations (*5*, *6*) and suggested as an explanation for the Evershed outflow in (*14*). The simulation shown here confirms this suggestion and demonstrates the convective nature of a fully developed penumbra.

The horizontal asymmetry of the convective flows is also manifest in the correlation of 0.42 between the corresponding flow component (v_x) and the brightness. We find that the rms of the outflowing velocity component (v_x) in the penumbra is much larger than the transverse component (v_y) (perpendicular to the filament direction), showing an asymmetry similar to that found by the scale analysis. The total rms velocity profile as a function of depth is very similar to its counterpart for undisturbed granulation, apart from a slightly higher peak value, confirming the physical similarity of convection in granulation and penumbra.

The mass flux and energy flux show similar properties with respect to the length scales and asymmetry (*8*), indicating that most of the outflowing material emerges, turns over, and descends within the penumbra. In the deeper layers, there is some contribution (of the order of 10 to 20%) to both energy and mass fluxes by the large-scale flow cell surrounding the sunspots.

The analysis of our simulations indicates that granulation and penumbral flows are similar with regard to energy transport; the asymmetry between the horizontal directions and the reduced overall energy flux reflect the constraints imposed on the convective motions by the presence of a strong and inclined magnetic field. The development of systematic outflows is a direct consequence of the anisotropy, and the similarities between granulation and penumbral flows strongly suggest that driving the Evershed flow does not require physical processes that go beyond the combination of convection and anisotropy introduced by the magnetic field. Weaker laterally overturning flows perpendicular to the main filament direction explain the apparent twisting motions observed in some filaments (*15*, *15*, *16*) and lead to a weakening of the magnetic field in the flow channels through flux expulsion (*6*).

Although our simulation of large sunspots is realistic in terms of relevant physics, it does not faithfully reproduce all aspects of the morphology of observed penumbral filaments. The penumbral regions are considerably more extended than in previous local simulations, but they are still somewhat subdued, probably owing to the proximity of the periodic boundaries. The filaments in the inner penumbrae appear to be too fragmented, and short, dark lanes along bright filaments (*17*) form only occasionally, likely a consequence of the still-limited spatial resolution of the simulation. Lastly, the initial condition of the magnetic field underlying the sunspot is quite arbitrary, owing to our ignorance of the subsurface structure of sunspots. Notwithstanding these limitations, the present simulations are consistent with observations of global sunspot properties, penumbral structure, and systematic radial outflows. These and earlier simulations (*5*, *6*, *10*) suggest a unified physical explanation for umbral dots as well as inner and outer penumbrae in terms of magnetoconvection in a magnetic field with varying inclination. Furthermore, a consistent physical picture of all observational characteristics of sunspots and their surroundings is now emerging.

References and Notes

1. S. K. Solanki, *Astron. Astrophys. Rev.* **11**, 153 (2003).
2. J. H. Thomas, N. O. Weiss, *Annu. Rev. Astron. Astrophys.* **42**, 517 (2004).
3. J. Evershed, *Mon. Not. R. Astron. Soc.* **69**, 454 (1909).
4. J. H. Thomas, N. O. Weiss, *Sunspots and Starspots* (Cambridge Univ. Press, Cambridge, 2008).
5. T. Heinemann, Å. Nordlund, G. B. Scharmer, H. C. Spruit, *Astrophys. J.* **669**, 1390 (2007).
6. M. Rempel, M. Schüssler, M. Knölker, *Astrophys. J.* **691**, 640 (2009).
7. M. Kubo, T. Shimizu, S. Tsuneta, *Astrophys. J.* **659**, 812 (2007).
8. More detailed information about the physical model, the numerical code, and the simulation setup is available as supporting material on *Science* Online.
9. R. Keppens, V. Martínez Pillet, *Astron. Astrophys.* **316**, 229 (1996).
10. M. Schüssler, A. Vögler, *Astrophys. J. Lett.* **641**, L73 (2006).
11. D. Dialetis, P. Mein, C. E. Alissandrakis, *Astron. Astrophys.* **147**, 93 (1985).
12. J. Sánchez Almeida, I. Márquez, J. A. Bonet, I. Domínguez Cerdeña, *Astrophys. J.* **658**, 1357 (2007).
13. L. R. Bellot Rubio, R. Schlichenmaier, A. Tritschler, *Astron. Astrophys.* **453**, 1117 (2006).
14. G. B. Scharmer, Å. Nordlund, T. Heinemann, *Astrophys. J. Lett.* **677**, L149 (2008).
15. K. Ichimoto *et al.*, *Science* **318**, 1597 (2007).
16. V. Zakharov, J. Hirzberger, T. Riethmüller, S. Solanki, P. Kobel, *Astron. Astrophys.* **488**, L17 (2008).
17. G. B. Scharmer, B. V. Gudiksen, D. Kiselman, M. G. Löfdahl, L. H. M. Rouppe van der Voort, *Nature* **420**, 151 (2002).

18. High-performance computing resources were provided by NCAR's Computational and Information Systems Laboratory. NCAR is sponsored by NSF.

Supporting Online Material
www.sciencemag.org/cgi/content/full/1173798/DC1
Materials and Methods
SOM Text
Figs. S1 to S4
References
Movies S1 and S2

19 March 2009; accepted 8 June 2009
Published online 18 June 2009;
10.1126/science.1173798
Include this information when citing this paper.

Quantum Walk in Position Space with Single Optically Trapped Atoms

Michal Karski,* Leonid Förster, Jai-Min Choi, Andreas Steffen, Wolfgang Alt, Dieter Meschede, Artur Widera*

The quantum walk is the quantum analog of the well-known random walk, which forms the ba
for models and applications in many realms of science. Its properties are markedly different
from the classical counterpart and might lead to extensive applications in quantum informat
science. In our experiment, we implemented a quantum walk on the line with single neutral a
by deterministically delocalizing them over the sites of a one-dimensional spin-dependent
optical lattice. With the use of site-resolved fluorescence imaging, the final wave function i
characterized by local quantum state tomography, and its spatial coherence is demonstrate
Our system allows the observation of the quantum-to-classical transition and paves the wa
applications, such as quantum cellular automata.

Interference phenomena with microscopic particles are a direct consequence of their quantum-mechanical wave nature (*1*–*5*). The prospect to fully control quantum properties of atomic systems has stimulated ideas to engineer quantum states that would be useful for applications in quantum information processing, for example, and also would elucidate fundamental questions, such as the quantum-to-classical transition (*6*). A prominent example of state engineering by controlled multipath interference is the quantum walk of a particle (*7*). Its classical counterpart, the random walk, is relevan
aspects of our lives, providing insight i
fields: It forms the basis for algorithm
scribes diffusion processes in physics
(*8*, *9*), such as Brownian motion, c
used as a model for stock market
Similarly, the quantum walk is expe

Institut für Angewandte Physik der Universit
straße 8, 53115 Bonn, Germany.

*To whom correspondence should be a
karski@uni-bonn.de (M.K.); widera@un

Realization of Quantum Walks with Negligible Decoherence in Waveguide Lattices

Hagai B. Perets,[1,*] Yoav Lahini,[1] Francesca Pozzi,[2] Marc Sorel,[2] Roberto Morandotti,[3] and Yaron Silberberg[1]
[1]*Faculty of Physics, The Weizmann Institute of Science, 76100 Rehovot, Israel*
[2]*Department of Electronics & Electrical Engineering, University of Glasgow, Glasgow G12 8QQ, Scotland, United Kingdom*
[3]*Institute National de la Recherche Scientifique, Universitá du Quebec, Varennes, Quebec J3X 1S2, Canada*

(Received 24 September 2007; published 2 May 2008)

Quantum random walks are the quantum counterpart of classical random walks, and were recently studied in the context of quantum computation. Physical implementations of quantum walks have only been made in very small scale systems severely limited by decoherence. Here we show that the propagation of photons in waveguide lattices, which have been studied extensively in recent years, are essentially an implementation of quantum walks. Since waveguide lattices are easily constructed at large scales and display negligible decoherence, they can serve as an ideal and versatile experimental playground for the study of quantum walks and quantum algorithms. We experimentally observe quantum walks in large systems (~ 100 sites) and confirm quantum walks effects which were studied theoretically, including ballistic propagation, disorder, and boundary related effects.

DOI: 10.1103/PhysRevLett.100.170506

PACS numbers: 03.67.Lx, 05.40.Fb, 42.25.Dd, 42.50.Xa

In classical random walks, a particle starting from an initial site on a lattice randomly chooses a direction, and then moves to a neighboring site accordingly. This process is repeated until some chosen final time. This simple random walk scheme is known to be described by a Gaussian probability distribution of the particle position, where the average absolute distance of the particle from the origin grows as the square root of time. First suggested by Feynman [1] the term *quantum* random walks was defined to describe the random walk behavior of a quantum particle. The coherent character of the quantum particle plays a major role in its dynamics, giving rise to markedly different behavior of quantum walks (QWs) compared with classical ones. For example, in periodic systems, the quantum particle propagates much faster than its classical counterpart, and its distance from the origin grows linearly with time (ballistic propagation) rather then diffusively [2]. In disordered systems, the expansion of the quantum mechanical wave-function can be exponentially suppressed even for infinitesimal amount of disorder, while such suppression does not occur in classical random walks.

In recent years QWs have been extensively studied theoretically [2] and have been used to devise new quantum computation algorithms [3]. Both discrete and continuous time QWs (DQWs; CQWs) [4–6] have been studied. In DQWs the quantum particle hops between lattice sites in discrete time steps, while in CQW the probability amplitude of the particle leaks continuously to neighboring sites. Experimentally, many methods have been suggested for the implementation of DQWs (see [2]), but only a small scale system consisting of a few states was implemented, using linear optical elements [7]. For CQWs, a few suggestions have been made [8,9], yet only one experimental method have been implemented by realizing a small scale cyclic system (4 states) using a nuclear magnetic resonance system [10]. Such systems are difficult to scale to much larger configurations. Moreover, even at these very small scales, errors attributed to decoherence have been observed.

Here we suggest a very different implementation of CQWs using optical waveguide lattices. These systems have been studied extensively in recent years [11], but not in the context of QWs and quantum algorithms. We show that these systems can serve as a unique and robust tool for the study of CQWs. For this purpose we demonstrate three fundamental QW effects that have been theoretically analyzed in the QW literature. These include ballistic propagation in the largest system reported to date (~ 100 sites), the effects of disorder on QWs, and QWs with reflecting boundary conditions (related to Berry's "particle in a box" and quantum carpets [12,13]). Waveguide lattices can be easily realized with even larger scales than shown here (10^2–10^4 sites with current fabrication technologies), with practically no decoherence. The high level of engineering and control of these systems enable the study of a wide range of different parameters and initial conditions. Specifically it allows the implementation and study of a large variety of CQWs and show experimental observations of their unique behavior.

The CQW model was first suggested by Farhi and Gutmann [6], where the intuition behind it comes from continuous time classical Markov chains. In the classical random walk on a graph, a step can be described by a matrix M which transforms the probability distribution for the particle position over the graph nodes (sites). The entries of the matrix $M_{j,k}$ give the probability to go from site j to site k in one step of the walk. The idea was to carry this construction over to the quantum case, where the *Hamiltonian* of the process is used as the generator matrix. The system is evolved using $U(t) = \exp(-iHt)$. If we start in some initial state $|\Psi_{in}\rangle$, evolve it under U for a time T and measure the positions of the resulting state, we obtain a

Momentum states

Consider an infinite path:

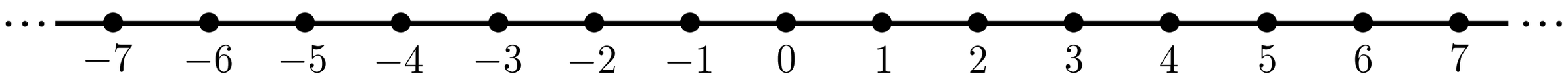

Hilbert space: $\mathrm{span}\{|x\rangle : x \in \mathbb{Z}\}$

Eigenstates of the adjacency matrix: $|\tilde{k}\rangle$ with

$$\langle x|\tilde{k}\rangle := e^{\mathrm{i}kx} \qquad k \in [-\pi, \pi)$$

Eigenvalue: $2\cos k$

Wave packets

A *wave packet* is a normalized state with momentum concentrated near a particular value k.

Example: $\frac{1}{\sqrt{L}} \sum_{x=1}^{L} e^{-\mathrm{i}kx} |x\rangle$ (large L)

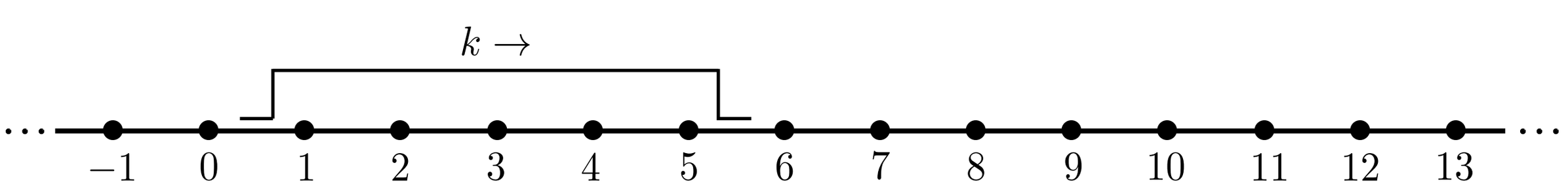

Propagation speed: $\left| \frac{\mathrm{d}E}{\mathrm{d}k} \right| = 2|\sin k|$

Scattering on graphs

Now consider adding semi-infinite lines to two vertices of an arbitrary finite graph.

Before:

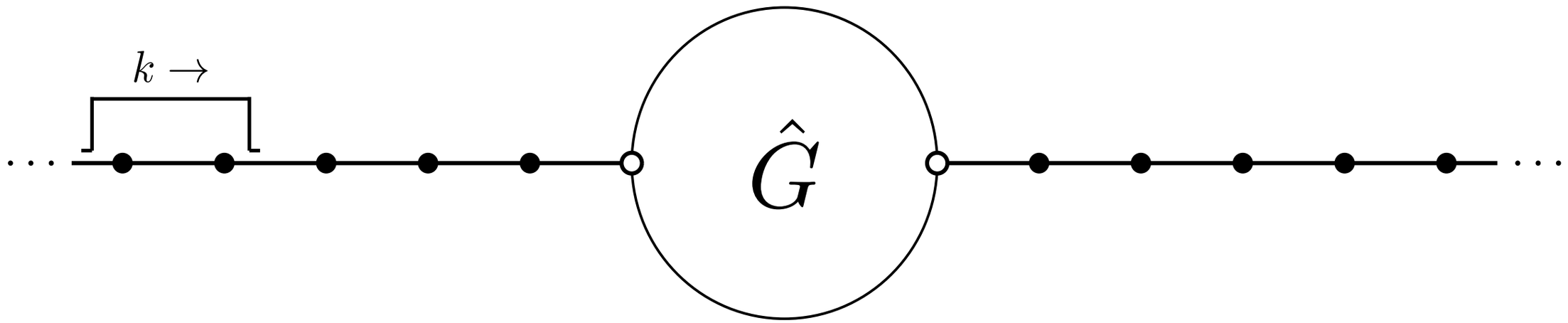

After:

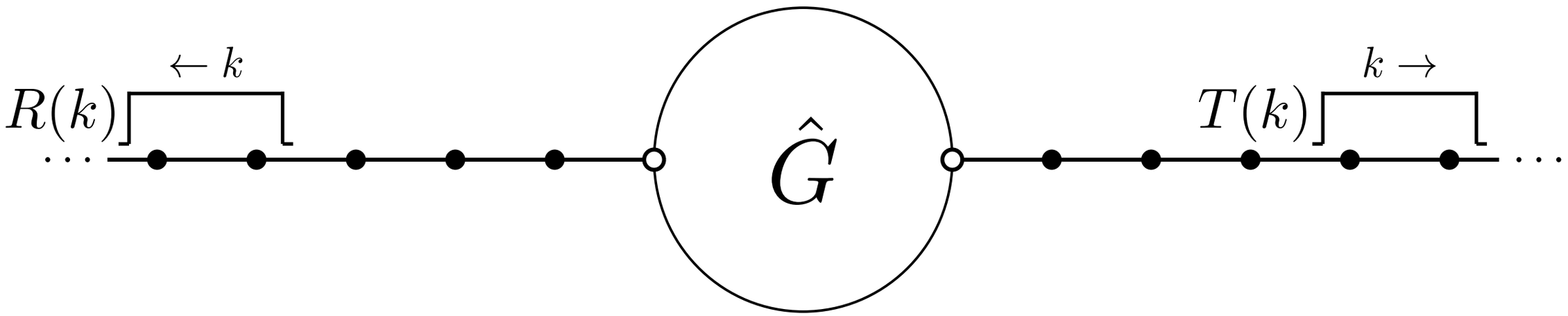

The S-matrix

This generalizes to any number N of semi-infinite paths attached to any finite graph.

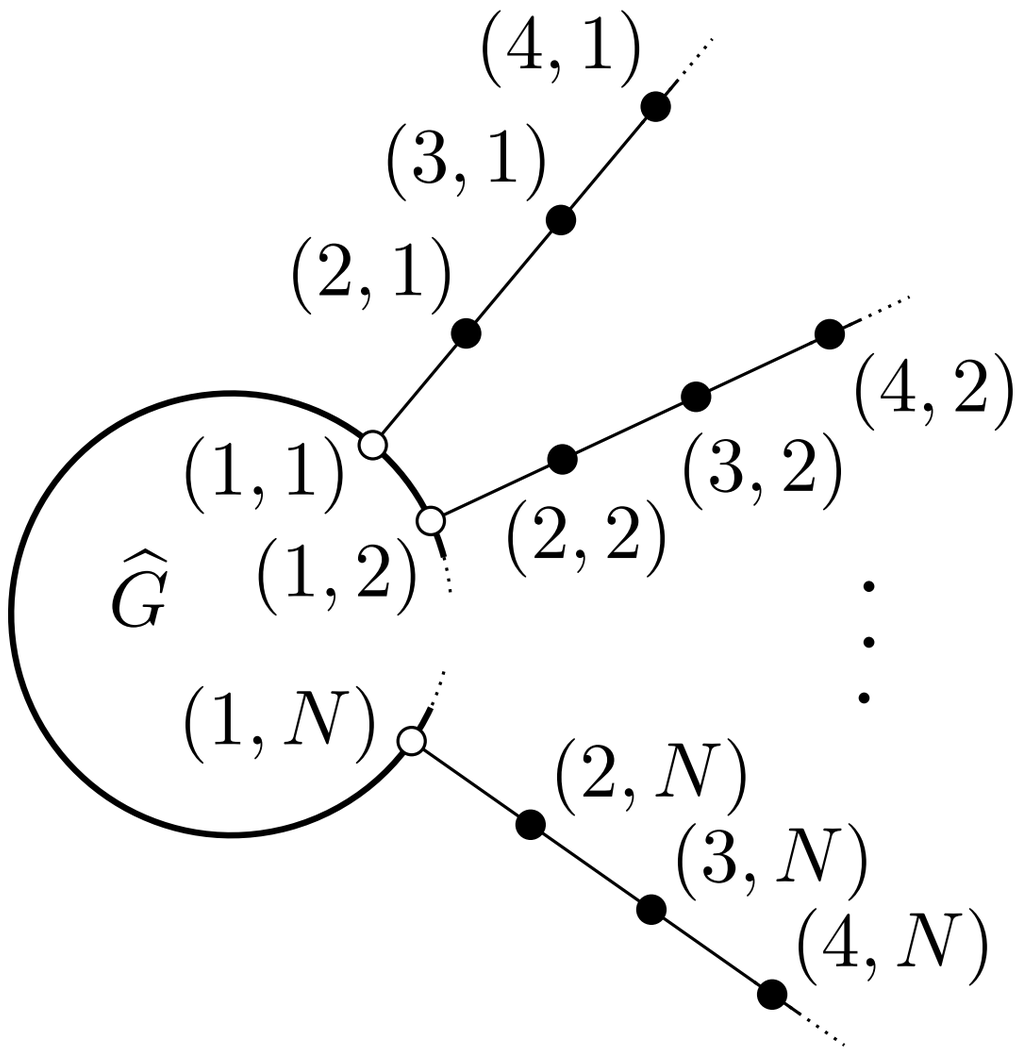

Incoming wave packets of momentum near k are mapped to outgoing wave packets (of the same momentum) with amplitudes corresponding to entries of an $N \times N$ unitary matrix $S(k)$, called the S-matrix.

Encoding a qubit

Encode quantum circuits into graphs.

Computational basis states correspond to paths ("quantum wires").

For one qubit, use two wires ("dual-rail encoding"):

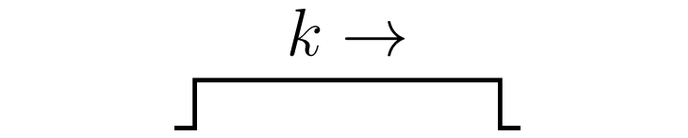

encoded $|0\rangle$

encoded $|1\rangle$

Fix some value of the momentum (e.g., $k = \pi/4$).

Quantum information propagates from left to right at constant speed.

Implementing a single-qubit gate

To perform a gate, design a graph whose S-matrix implements the desired transformation U at the momentum used for the encoding.

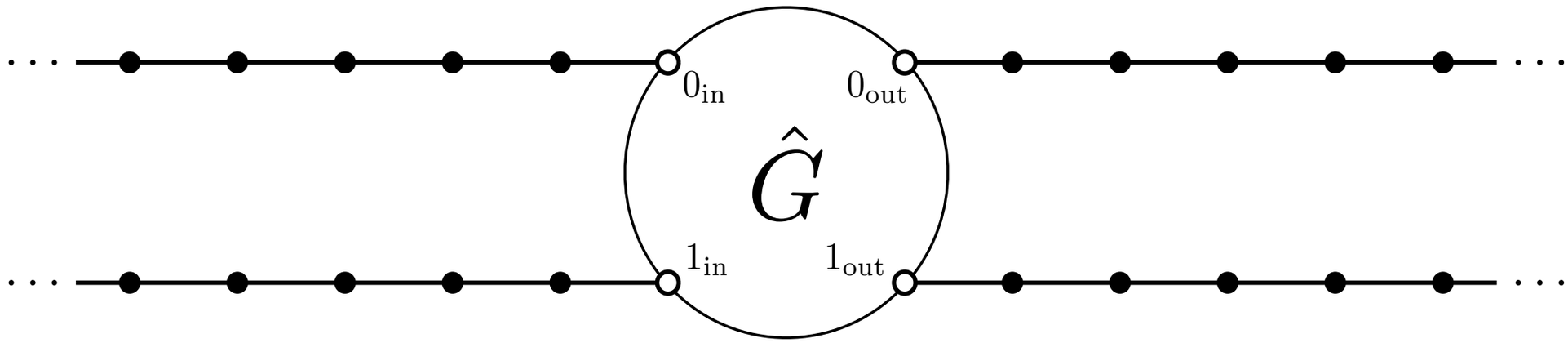

$$S(k) = \begin{pmatrix} 0 & V \\ U & 0 \end{pmatrix}$$

Universal set of single-qubit gates

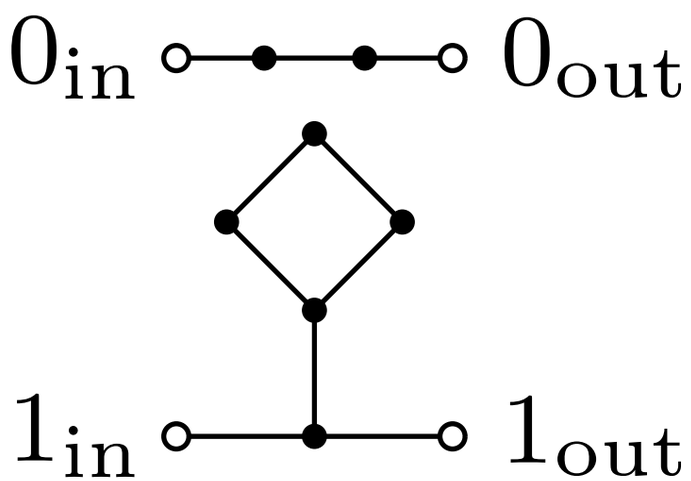

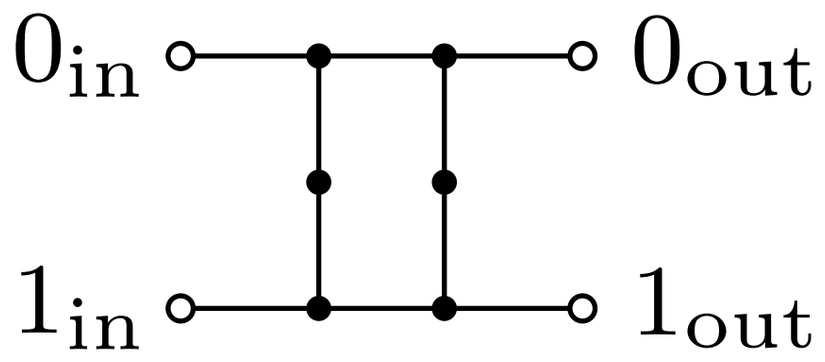

$$\begin{pmatrix} 1 & 0 \\ 0 & \sqrt{\mathrm{i}} \end{pmatrix} \qquad\qquad -\frac{1}{\sqrt{2}} \begin{pmatrix} \mathrm{i} & 1 \\ 1 & \mathrm{i} \end{pmatrix}$$

momentum for logical states: $k = \pi/4$

Two-particle scattering

In general, multi-particle scattering is complicated.

But scattering of indistinguishable particles on an infinite path is simple.

Before:

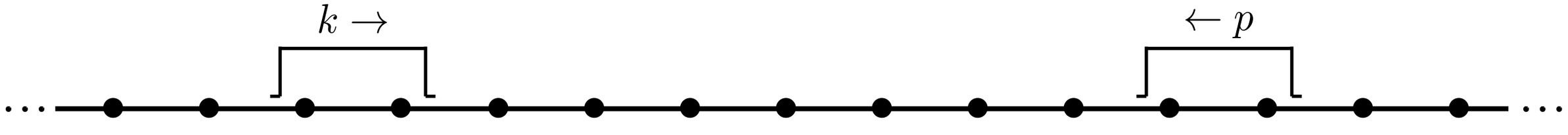

After:

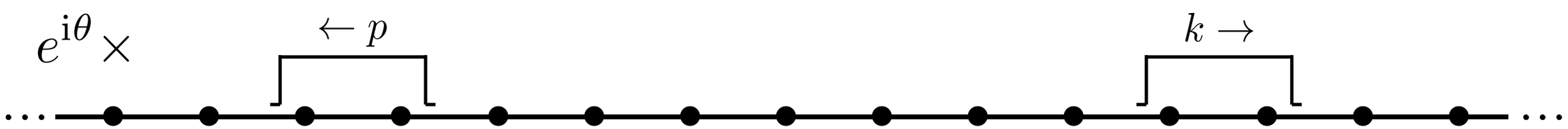

Phase θ depends on momenta and interaction details.

Momentum switch

To selectively induce the two-particle scattering phase, we route particles depending on their momentum.

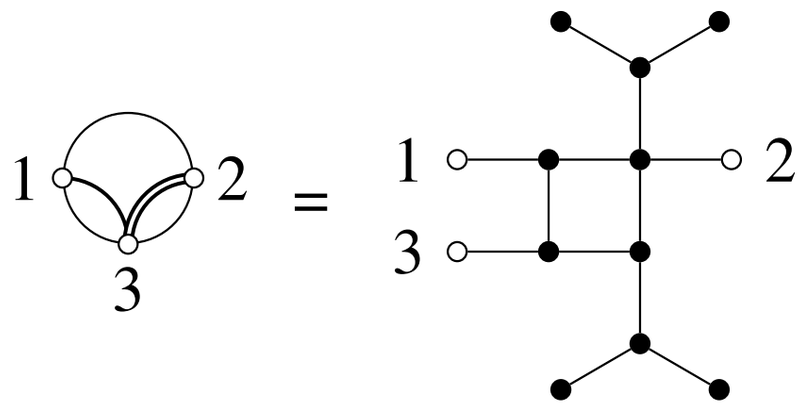

Particles with momentum $\pi/4$ follow the single line.

Particles with momentum $\pi/2$ follow the double line.

Controlled phase gate

Computational qubits have momentum $\pi/4$. Introduce a "mediator qubit" with momentum $\pi/2$. We can perform an entangling gate with the mediator qubit.

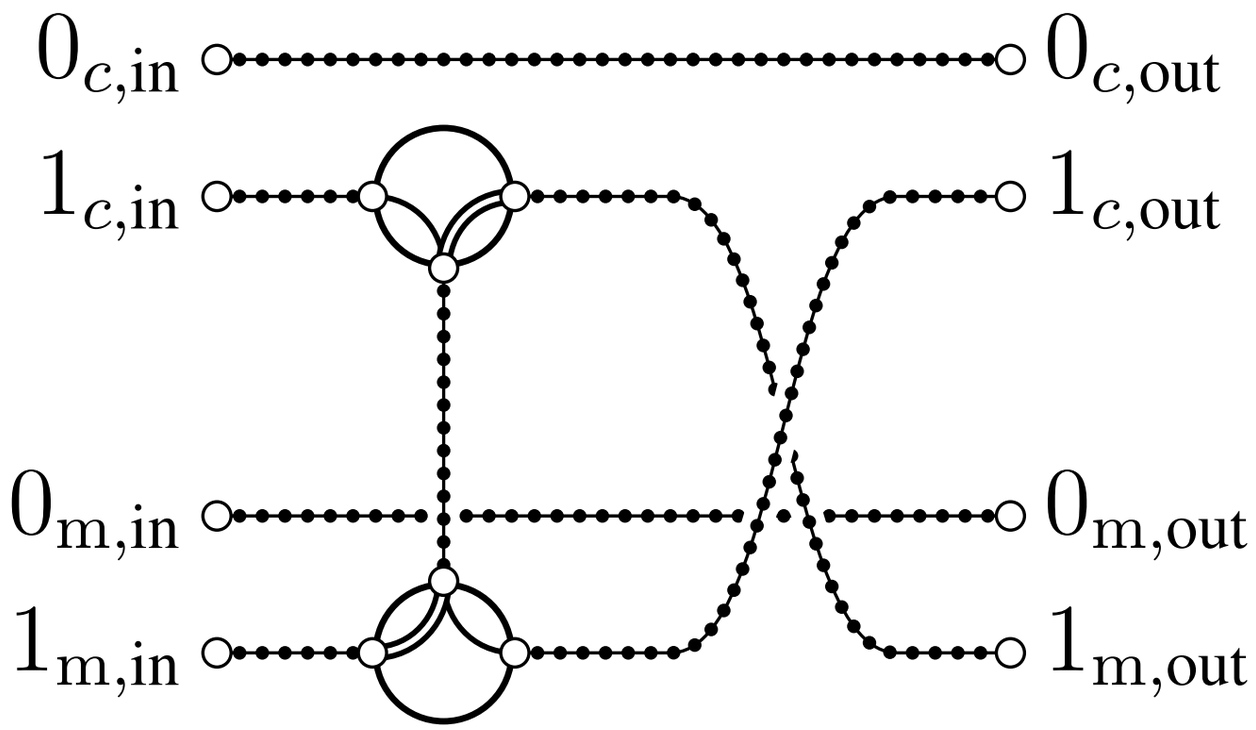

$$\mathrm{C}\theta = \begin{pmatrix} 1 & 0 & 0 & 0 \\ 0 & 1 & 0 & 0 \\ 0 & 0 & 1 & 0 \\ 0 & 0 & 0 & e^{\mathrm{i}\theta} \end{pmatrix}$$

Hadamard on mediator qubit

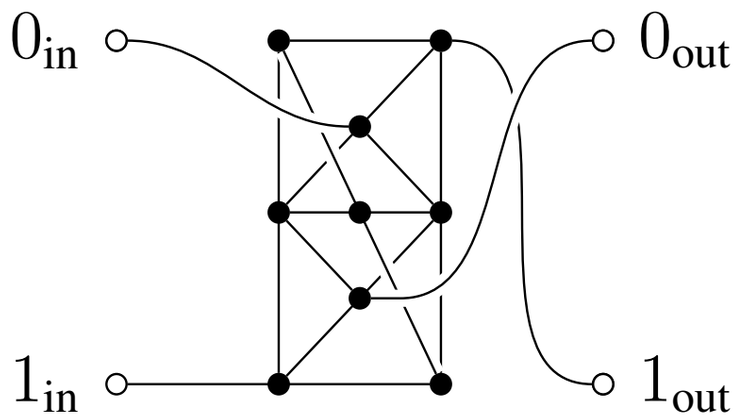

[Blumer-Underwood-Feder 11]

Proving an error bound

Proof ideas:

- With long enough incoming square wave packets (length L), the outgoing wave packets are well-approximated by the effect of the S-matrix (error $O(L^{-1/4})$). We prove this for single-particle scattering (for any graph) and for two-particle scattering on an infinite path.
- Truncation Lemma: If the state is well-approximated by one that is well-localized to some region, then changing how the Hamiltonian acts outside that region has little effect.

Theorem: The error can be made arbitrarily small with $L = \mathrm{poly}(n, g)$.

Example: For Bose-Hubbard model, $L = O(n^{12} g^4)$ suffices.

Open questions

- Improved error bounds
- Simplified initial state
- Are generic interactions universal for distinguishable particles?
- New quantum algorithms
- Experiments
- Fault tolerance

The Bose-Hubbard model is QMA-compete

arXiv:1311.3297

Quantum Merlin-Arthur

QMA: the quantum analog of NP

Merlin wants to prove to Arthur that some statement is true.

Merlin

quantum proof $|\psi\rangle$

Arthur

efficient quantum verification circuit

- If the statement is true, there exists a $|\psi\rangle$ that Arthur will accept with probability at least 2/3.
- If the statement is false, any $|\psi\rangle$ will be rejected by Arthur with probability at least 2/3.

Complexity of ground energy problems

- k-Local Hamiltonian problem: QMA-complete for $k \geq 2$ [Kempe, Kitaev, Regev 2006]
- Quantum k-SAT (is there a frustration-free ground state?): in P for $k=2$; QMA_1-complete for $k \geq 3$ [Bravyi 2006; Gosset, Nagaj 2013]
- Stoquastic k-local Hamiltonian problem: in AM [Bravyi et al. 2006]
- Fermion/boson problems: QMA-complete [Liu, Christandl, Verstraete 2007; Wei, Mosca, Nayak 2010]
- 2-local Hamiltonian on a grid: QMA-complete [Oliveira, Terhal 2008]
- 2-local Hamiltonian on a line of qudits: QMA-complete [Aharonov, Gottesman, Irani, Kempe 2009]
- Hubbard model on a 2d grid with a site-dependent magnetic field: QMA-complete [Schuch, Verstraete 2009]
- Heisenberg and XY models with site-dependent couplings: QMA-complete [Cubitt, Montanaro 2013]

Bose-Hubbard Hamiltonian is QMA-complete

Bose-Hubbard model on G:

$$H_G = t_{\text{hop}} \sum_{u,v \in V(G)} A(G)_{uv} a_u^\dagger a_v + J_{\text{int}} \sum_{v \in V(G)} \hat{n}_v(\hat{n}_v - 1)$$

Theorem: Determining whether the ground energy for n particles on the graph G is less than $ne_1 + \epsilon$ or more than $ne_1 + 2\epsilon$ is QMA-complete, where e_1 is the 1-particle ground energy.

- Fixed movement and interaction terms ($A(G)$ is a 0-1 matrix)
- Applies for any fixed $t_{\text{hop}}, J_{\text{int}} > 0$
- It is QMA-hard even to determine whether the instance is approximately frustration free
- Analysis does not use perturbation theory

Dependence on signs of coefficients

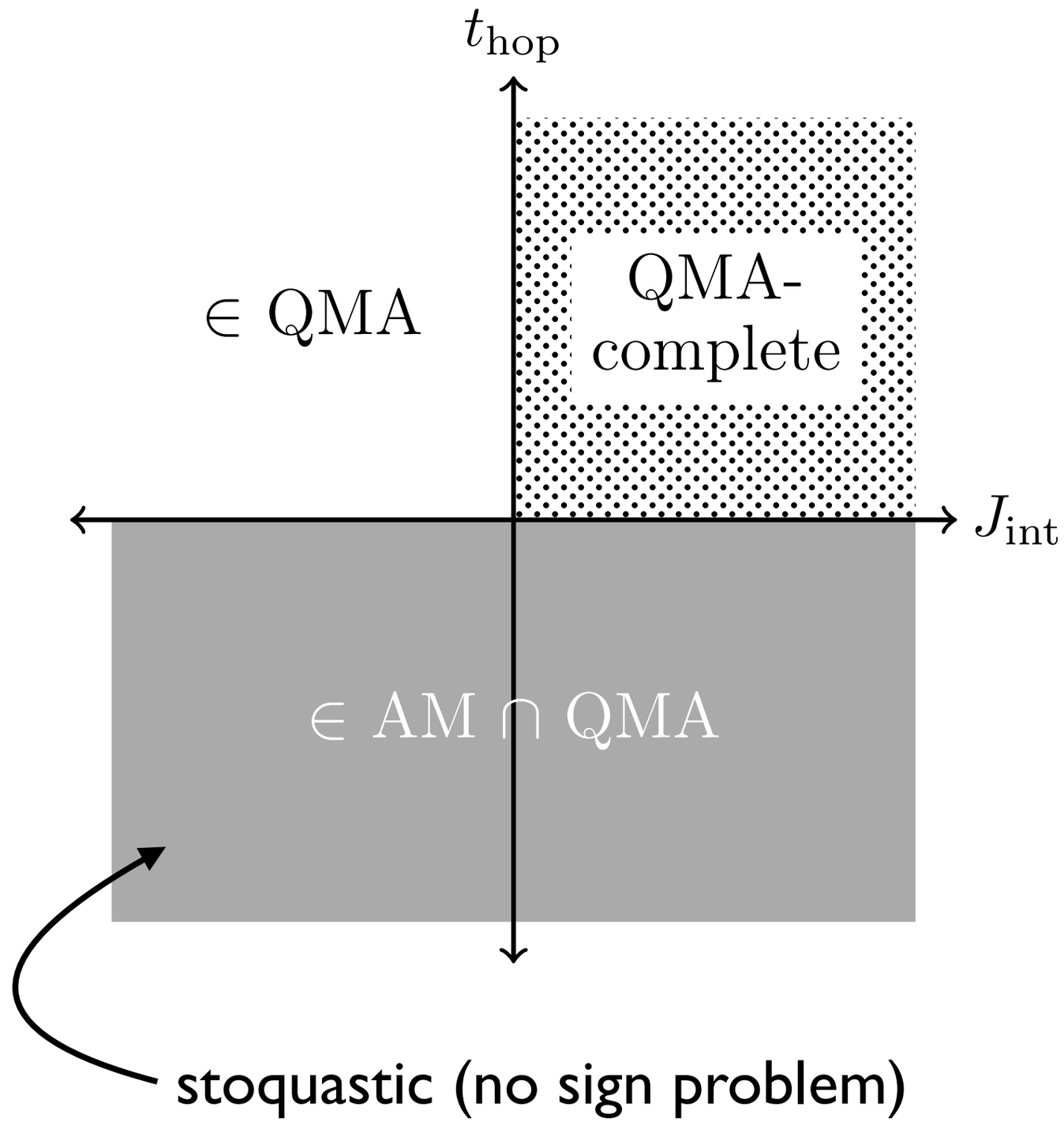

XY model

We encode computations in the subspace with at most one boson per site ("hard-core bosons")

Thus we can translate our results to spin systems, giving a generalization of the XY model on a graph:

$$\sum_{\substack{A(G)_{ij}=1 \\ i \neq j}} \frac{\sigma_x^i \sigma_x^j + \sigma_y^i \sigma_y^j}{2} + \sum_{A(G)_{ii}=1} \frac{1 - \sigma_z^i}{2}$$

Theorem: Approximating the ground energy in the sector with magnetization $\sum_i \frac{1-\sigma_z^i}{2} = n$ is QMA-complete.

Containment in QMA

Ground energy problems are usually in QMA

Strategy:

- Merlin provides the ground state
- Arthur measures the energy using phase estimation and Hamiltonian simulation

Only one small twist for boson problems: project onto the symmetric subspace

The quantum Cook-Levin Theorem

Theorem: Local Hamiltonian is QMA-complete [Kitaev 99]

Consider a QMA verification circuit $U_t \dots U_2 U_1$ with witness $|\psi\rangle$

The Feynman Hamiltonian

$$H = \sum_{j=1}^{t} (I \otimes |j\rangle\langle j| + I \otimes |j-1\rangle\langle j-1| - U_j \otimes |j\rangle\langle j-1| - U_j^\dagger \otimes |j-1\rangle\langle j|)$$

has ground states $|\mathrm{hist}_\psi\rangle = \frac{1}{\sqrt{t+1}} \sum_{j=0}^{t} U_j \dots U_1 |\psi\rangle \otimes |j\rangle$

- Implement the "clock" using local terms
- Add a term penalizing states with low acceptance probability

Single-qubit gates

Construct a graph encoding a universal set of single-qubit gates in the single-particle sector:

- Start from Feynman-Kitaev Hamiltonian for a particular sequence of gates
- Obtain matrix elements {-1,0,+1} by careful choice of gate set and scaling
- Remove negative entries using an ancilla

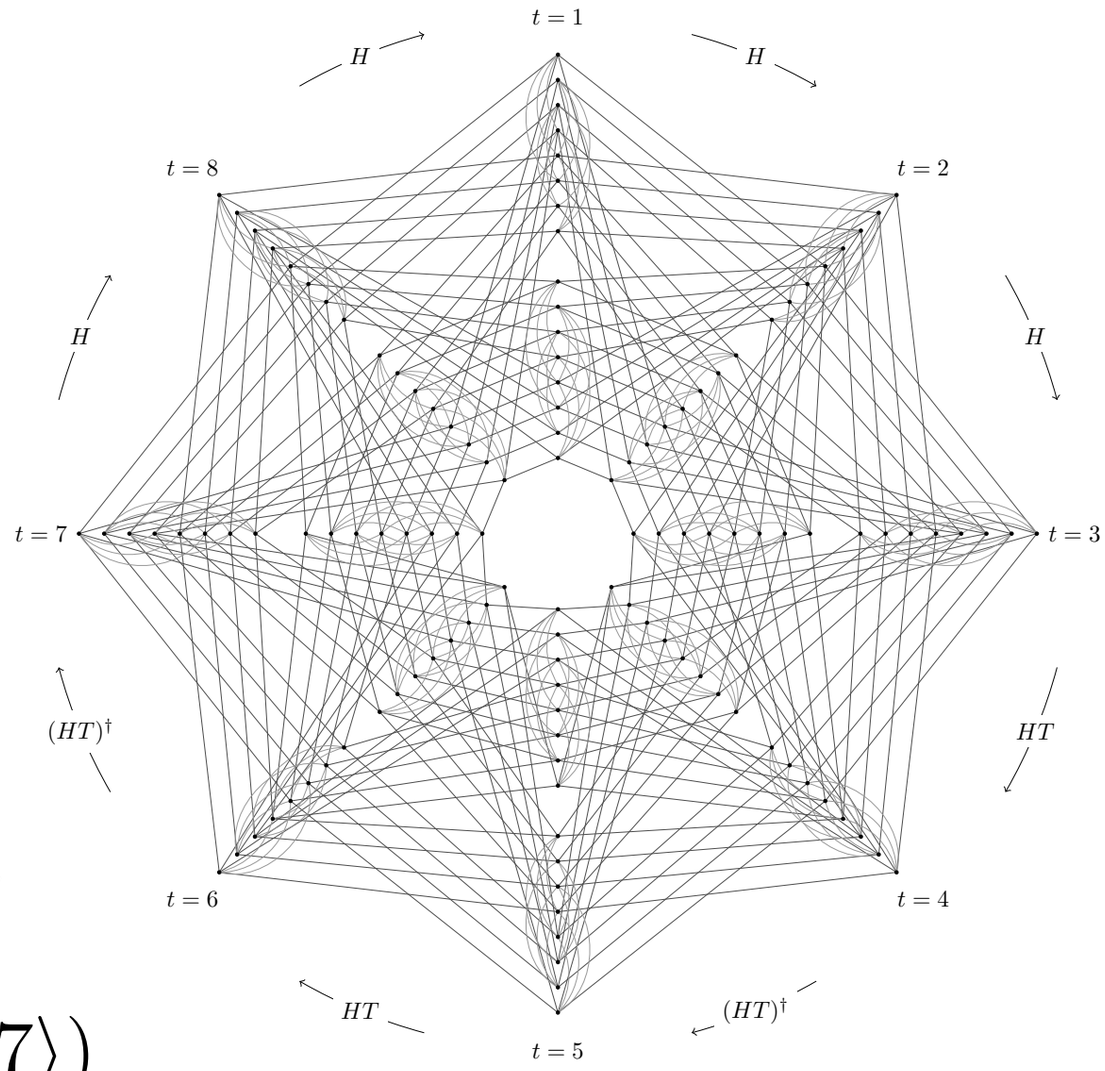

Ground state subspace is spanned by

$$|\psi_{z,0}\rangle = \frac{1}{\sqrt{8}}\big(|z\rangle(|1\rangle + |3\rangle + |5\rangle + |7\rangle) + H|z\rangle(|2\rangle + |8\rangle) + HT|z\rangle(|4\rangle + |6\rangle)\big)|\omega\rangle$$

$$|\psi_{z,1}\rangle = |\psi_{z,0}\rangle^*$$

for $z \in \{0, 1\}$

some ancilla state

Two-qubit gates

Two-qubit gate gadgets: 4096-vertex graphs built from 32 copies of the single-qubit graph, joined by edges and with some added self-loops

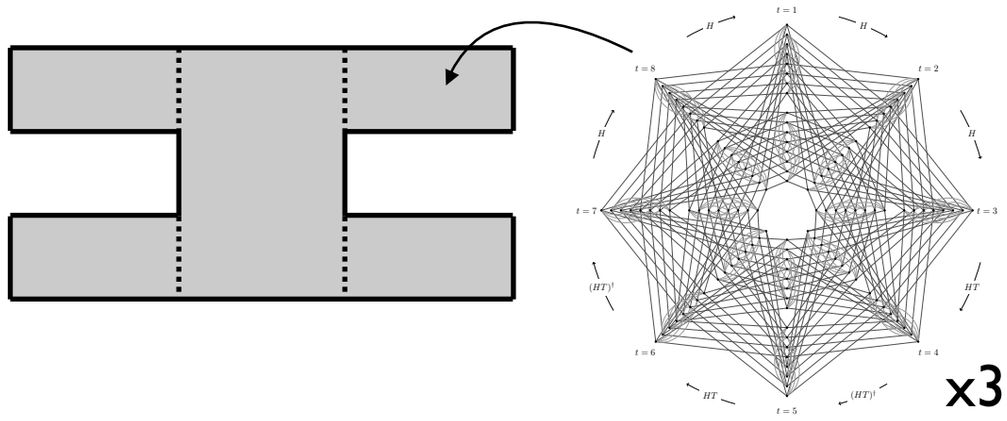

x32

Single-particle ground states are associated with one of two input regions or one of two output regions:

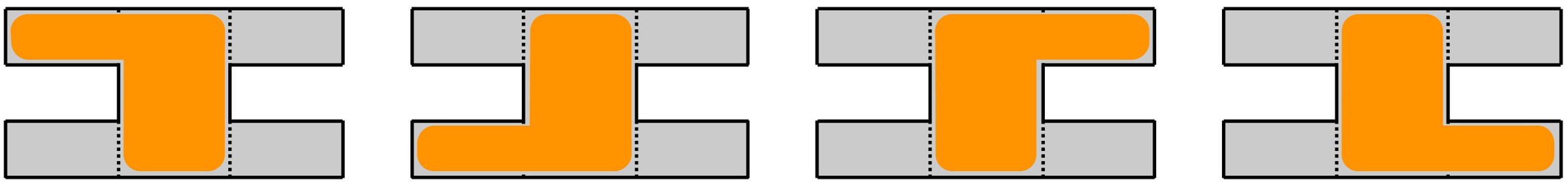

(States also carry labels associated with the logical state & complex conjugation.)

Two-particle ground states encode two-qubit computations:

$$\frac{1}{\sqrt{2}}\left(\left|\;\right\rangle \otimes |\psi\rangle + \left|\;\right\rangle \otimes U|\psi\rangle\right)$$

Constructing a verification circuit

Connect two-qubit gate gadgets to implement the whole verification circuit, e.g.:

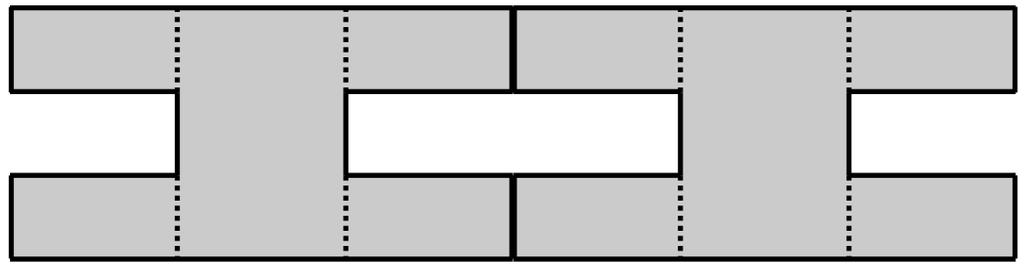

Some multi-particle ground states encode computations:

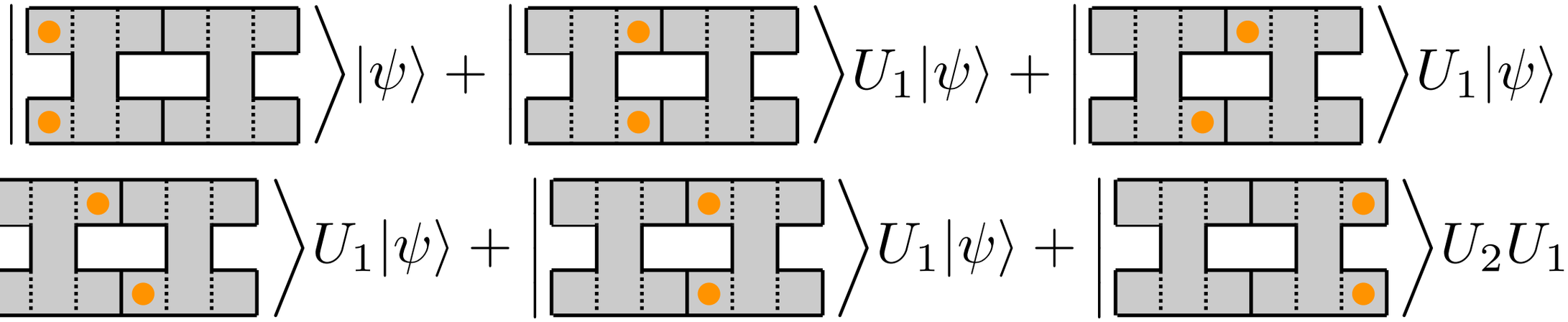

But there are also ground states that do not encode computations (two particles for the same qubit; particles not synchronized).

To avoid this, we introduce a way of enforcing *occupancy constraints*, forbidding certain kinds of configurations. We establish a promise gap using nonperturbative spectral analysis (no large coefficients).

Open questions

- Remove self-loops?
- Complexity of other models of multi-particle quantum walk
  - Attractive interactions
  - Negative hopping strength (stoquastic; is it AM-hard?)
  - Bosons or fermions with nearest-neighbor interactions
  - Unrestricted particle number
- Complexity of other quantum spin models defined on graphs
  - XY model
  - Antiferromagnetic Heisenberg model